

SYNTHESIS AND PROPERTIES  
OF INORGANIC COMPOUNDSVaporization and Thermodynamic Properties of the CeO<sub>2</sub>–TiO<sub>2</sub>  
System by Knudsen Effusion Mass SpectrometryS. M. Shugurov<sup>a,\*</sup>, O. A. Zhinkina<sup>a</sup>, D. A. Repin<sup>b</sup>, E. A. Balabanova<sup>b</sup>, and S. I. Lopatin<sup>b</sup><sup>a</sup> Institute of Chemistry, St. Petersburg State University, St. Petersburg, 198504 Russia<sup>b</sup> Institute of Silicate Chemistry, Russian Academy of Sciences, St. Petersburg, 199034 Russia

\*e-mail: s.shugurov@spbu.ru

Received July 21, 2025; revised October 20, 2025; accepted October 22, 2025

**Abstract**—Samples in the TiO<sub>2</sub>–CeO<sub>2</sub> system with CeO<sub>2</sub> concentrations ranging from 10 to 90 mol % were synthesized using the ceramic method. The phase composition of the obtained samples was determined by X-ray diffraction (XRD). Melting temperatures were measured by visual polythermal analysis. The composition and partial pressures of molecular vapor species over the TiO<sub>2</sub>–CeO<sub>2</sub> system were determined across a wide range of condensed-phase compositions. For the melts in the studied system, component activities, Gibbs energies, and excess Gibbs energies were determined at 2150 K. It was shown that the system exhibits negative deviations from ideal behavior.

**Keywords:** vaporization, thermodynamic properties, Knudsen effusion mass spectrometry, ceria-titania system

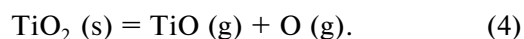
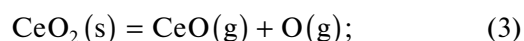
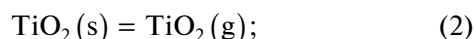
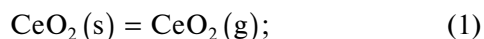
**DOI:** 10.1134/S0036023625602727

## INTRODUCTION

Ceramic materials based on cerium dioxide (CeO<sub>2</sub>) and titanium dioxide (TiO<sub>2</sub>) are of considerable interest due to a unique combination of functional properties, including photocatalytic activity [1, 2], luminescence [3], ion-exchange capability, and resistance to high-temperature degradation [4]. The development of complex oxide systems such as CeO<sub>2</sub>–TiO<sub>2</sub> makes it possible to modify the electronic structure and optimize the performance characteristics of materials, which is relevant for the design of catalysts, sensors, and solid oxide electrolytes.

The synthesis and operation of ceramic materials often involve high temperatures. This can cause preferential sublimation of the more volatile components, leading to irreversible changes in the composition of the condensed phase and, consequently, in its properties.

The high-temperature behavior of individual cerium and titanium dioxides has been investigated previously [5–10]. It has been shown that both oxides vaporize with partial dissociation in accordance with reactions (1)–(4):



At high temperatures, cerium and titanium dioxides may lose oxygen, transforming into Ce<sub>2</sub>O<sub>3</sub> [11] and Ti<sub>3</sub>O<sub>5</sub> [12], respectively.

The vaporization behavior of complex oxide systems containing cerium dioxide has been studied in several works [13–15]. These studies have determined the qualitative and quantitative composition of the vapor as a function of temperature and condensed-phase composition, and have derived the corresponding thermodynamic characteristics. The CeO<sub>2</sub>–ZrO<sub>2</sub> [13], CeO<sub>2</sub>–Gd<sub>2</sub>O<sub>3</sub> [14], and CeO<sub>2</sub>–Y<sub>2</sub>O<sub>3</sub> [15] systems are characterized by preferential sublimation of cerium oxide and a negative deviation from ideal behavior. In ref. [16], the activities of cerium dioxide were determined for three compositions in the CeO<sub>2</sub>–TiO<sub>2</sub>–ZrO<sub>2</sub> system.

The aim of this work is to study the vaporization processes and determine the thermodynamic characteristics of the TiO<sub>2</sub>–CeO<sub>2</sub> system over a wide range of component concentrations. This research continues our systematic investigation into the vaporization behavior and thermodynamic properties of oxygen ceramics containing cerium (IV) oxide.

## EXPERIMENTAL SECTION

A series of nine samples in the TiO<sub>2</sub>–CeO<sub>2</sub> system (10–90 mol.% CeO<sub>2</sub> in 10 mol.% steps) was prepared by the ceramic route. High-purity (99.9%) CeO<sub>2</sub> and TiO<sub>2</sub> of analytical grade were used as starting materi-

als. Sample homogenization was carried out using a PM100 planetary mill (Retsch GmbH, Germany). After mixing and prolonged grinding, the powder mixtures were pressed into pellets 10 mm in diameter and 5 mm in height. The pressed pellets were placed in a muffle furnace and annealed at 1400°C for 22.5 h. The samples were then cooled inside the furnace.

The phase composition of the annealed samples was examined by powder X-ray diffraction (XRD) using D8 Discover diffractometer (Bruker, Germany) with  $\text{CuK}\alpha$  radiation ( $\lambda = 1.5406 \text{ \AA}$ ). Qualitative phase identification was performed using the Powder Diffraction File database (PDF-2, 2012). Quantitative phase analysis was carried out by the Rietveld method using TOPAS 5.0 software (Bruker, Germany) and structural data for each phase taken from the ICDD database. The scanning step and counting time were adjusted to ensure reliable refinement with the applied software.

Melting temperatures of the samples were measured by visual polythermal analysis using a high-temperature microscope [17]. The investigated sample was fixed on a loop with a diameter of 0.25 mm made of iridium wire. The wire with the sample was heated by alternating electric current regulated by a LATR-9 autotransformer. The temperature was measured using a Platinum/platinum–rhodium thermocouple. Instrument calibration was performed by determining the melting temperatures of reference substances.  $\text{Al}_2\text{O}_3$ ,  $\text{SiO}_2$ ,  $\text{TiO}_2$ ,  $\text{K}_2\text{SO}_4$ ,  $\text{SrTiO}_3$ , and  $\text{BaTiO}_3$  were used as standards. For each sample, melting temperature measurements were performed twice to obtain more reliable values. During heating, the sample was observed using a high-temperature microscope until melting occurred and the sample completely filled the loop in the form of a thin film transparent to polarized light, or until failure of the iridium wire at 2446°C. The voltages applied to the wire at the onset and completion of melting were recorded. These data were used to determine the melting temperature from a calibration curve. The uncertainty in temperature determination did not exceed  $\pm 20^\circ\text{C}$ .

The oxidation states of the elements were determined by X-ray photoelectron spectroscopy (XPS) using a combined Auger, X-ray, and ultraviolet photoelectron spectrometer (Thermo Fisher Scientific ESCA-lab 250Xi, USA).

Vaporization processes and thermodynamic properties of the  $\text{TiO}_2$ – $\text{CeO}_2$  system were studied by high-temperature differential mass spectrometry using an MS-1301 mass spectrometer (Special Design Bureau of Analytical Instrument Engineering, USSR) with an ionizing voltage of 30 V. The samples were vaporized from a tungsten twin Knudsen effusion cell. One compartment of the cell was loaded with the investigated sample, while the second (reference) compartment was alternately loaded with individual  $\text{CeO}_2$  or  $\text{Ti}_3\text{O}_5$ . The cell was heated by electron bombardment. The

temperature was measured using an EOP-66 optical pyrometer (“Pribor”, Ukrainian SSR) with an accuracy of  $\pm 10 \text{ K}$  in the temperature range of 1700–2500 K. Prior to the experiments, the apparatus was calibrated using the vapor pressure of  $\text{CaF}_2$  [18].

The activities of cerium dioxide and titanium dioxide in the condensed phase were determined using Eqs. (5) and (6), respectively:

$$a(\text{CeO}_2) = \frac{p(\text{CeO}_2)}{p_0(\text{CeO}_2)} = \frac{I(\text{CeO}_2^+)}{I_0(\text{CeO}_2^+)}, \quad (5)$$

$$a(\text{TiO}_2) = \frac{p(\text{TiO}_2)}{p_0(\text{TiO}_2)} = \frac{I(\text{TiO}_2^+)}{I_0(\text{TiO}_2^+)}, \quad (6)$$

where  $p$ ,  $p_0$ ,  $I^+$ , and  $I_0^+$  are the partial pressures and ion current intensities in the mass-spectra measured over the sample and over the individual cerium and titanium oxides.

In Eqs. (5) and (6), the partial pressures of cerium and titanium oxides were replaced by quantities proportional to them, namely the ion current intensities, in accordance with the following relation:

$$p = kIT, \quad (7)$$

where  $k$  is the instrumental sensitivity coefficient and  $T$  is the temperature (K).

## RESULTS AND DISCUSSION

The results of the phase analysis of the synthesized samples are presented in Table 1.

Analysis of the phase composition of the investigated samples at room temperature revealed that all synthesized samples contain a stable  $\text{CeTi}_2\text{O}_6$  phase, regardless of the initial molar ratio of the starting components. Its content varies depending on composition and ranges from 9 to 78%. The observed shifts in the  $\text{CeO}_2$  diffraction peaks relative to those of pure ceria indicate a distinct interaction between  $\text{CeO}_2$  and  $\text{TiO}_2$ , confirming their compatibility and the formation of solid solutions. Although room-temperature XRD revealed a multiphase composition, at the experimental temperature of 2150 K samples No. 2–5 existed as a homogeneous melt. Consequently, the room-temperature phase composition was disregarded in the thermodynamic analysis.

Due to the significant difference in volatility between  $\text{CeO}_2$  and  $\text{TiO}_2$  [19], the differential mass spectrometry method cannot be used to determine component activities across the entire composition range of the system. A complete thermodynamic description of the studied system can only be obtained within the homogeneity region by applying the Gibbs–Duhem equation to determine the activity of the less volatile component, while the activity of the second component is determined experimentally. Unfortunately, no phase diagram data for the  $\text{TiO}_2$ –

**Table 1.** Phase analysis of samples in the TiO<sub>2</sub>–CeO<sub>2</sub> system annealed at 1400°C in air for 22.5 h with subsequent furnace cooling

№ sample	Chemical composition (by synthesis), mol. fr.		Qualitative analysis	Quantitative analysis, %
	CeO <sub>2</sub>	TiO <sub>2</sub>		
1	0.1	0.9	CeTi <sub>2</sub> O <sub>6</sub> CeO <sub>2</sub> TiO <sub>2</sub>	19 3 78
2	0.2	0.8	CeTi <sub>2</sub> O <sub>6</sub> CeO <sub>2</sub> TiO <sub>2</sub>	44 4 52
3	0.3	0.7	CeTi <sub>2</sub> O <sub>6</sub> CeO <sub>2</sub> TiO <sub>2</sub>	67 10 23
4	0.4	0.6	CeTi <sub>2</sub> O <sub>6</sub> CeO <sub>2</sub> TiO <sub>2</sub>	75 23 2
5	0.5	0.5	CeTi <sub>2</sub> O <sub>6</sub> CeO <sub>2</sub> TiO <sub>2</sub>	55 42 3
6	0.6	0.4	CeTi <sub>2</sub> O <sub>6</sub> CeO <sub>2</sub>	43 57
7	0.7	0.3	CeTi <sub>2</sub> O <sub>6</sub> CeO <sub>2</sub>	32 68
8	0.8	0.2	CeTi <sub>2</sub> O <sub>6</sub> CeO <sub>2</sub>	20 80
9	0.9	0.1	CeTi <sub>2</sub> O <sub>6</sub> CeO <sub>2</sub>	9 91

CeO<sub>2</sub> system could be found in the literature. Therefore, the activities of the condensed-phase components were determined in the region of the homogeneous melt. To identify this region, melting temperatures of the samples were measured by visual polythermal analysis. The obtained values are presented in Table 2.

To monitor possible reduction of the dioxides during synthesis, the samples were examined by XPS. Analysis confirmed that titanium is present exclusively as Ti<sup>4+</sup> in all samples. Cerium is present predominantly as Ce<sup>4+</sup>, with an admixture of Ce<sup>3+</sup> (11–15%) detected in all samples. This Ce<sup>3+</sup> content matches that found in the pure CeO<sub>2</sub> starting material. A slight increase in the relative Ce<sup>3+</sup> content is observed with decreasing molar fraction of CeO<sub>2</sub>. This trend, however, may be attributed to the reduced spectral resolution and the associated uncertainties in peak deconvolution.

It should be noted that the presence of Ce<sup>3+</sup> in the XPS spectra may result from partial surface reduction of cerium dioxide during XPS measurements, a phenomenon that has been repeatedly reported in the literature [20, 21]. In contrast to ref. [22], no broadening of the Ti peaks was observed for any of the samples, which may be attributed to differences in the synthesis method.

The mass spectra of the vapor over the CeO<sub>2</sub>–TiO<sub>2</sub> system in the 1900–2200 K range contained CeO<sup>+</sup>, CeO<sub>2</sub><sup>+</sup>, TiO<sup>+</sup>, and TiO<sub>2</sub><sup>+</sup> ions. To identify the molecular precursors of these ions, their appearance energies were measured using the vanishing ion current method. The obtained values were: CeO<sup>+</sup>(5.0), CeO<sub>2</sub><sup>+</sup>(9.5), TiO<sup>+</sup>(6.8) и TiO<sub>2</sub><sup>+</sup>(9.6) eV. Inflection points were observed in the ionization efficiency (IE) curves for CeO<sup>+</sup> and TiO<sup>+</sup>, whereas no inflections were

**Table 2.** Melting temperatures of the samples in the TiO<sub>2</sub>–CeO<sub>2</sub> system determined by visual polythermal analysis

No. sample	Sample composition, mol %	Onset of melting, °C	Completion of melting, °C
1	10CeO <sub>2</sub> –90TiO <sub>2</sub>	2133	2193
2	20CeO <sub>2</sub> –80TiO <sub>2</sub>	1853	1958
3	30CeO <sub>2</sub> –70TiO <sub>2</sub>	1763	1763
4	40CeO <sub>2</sub> –60TiO <sub>2</sub>	1833	1853
5	50CeO <sub>2</sub> –50TiO <sub>2</sub>	1723	1853
6	60CeO <sub>2</sub> –40TiO <sub>2</sub>	1763	1813
7	70 CeO <sub>2</sub> –30TiO <sub>2</sub>	2143	2213
8	80CeO <sub>2</sub> –20TiO <sub>2</sub>	2413	2423
9	90CeO <sub>2</sub> –10TiO <sub>2</sub>	2493	2493

detected for CeO<sub>2</sub><sup>+</sup> and TiO<sub>2</sub><sup>+</sup>. The measured values are consistent, within experimental error, with the reported ionization energies of CeO, CeO<sub>2</sub>, TiO, and TiO<sub>2</sub> [23], indicating their molecular origin. The

nature of the CeO<sup>+</sup> and CeO<sub>2</sub><sup>+</sup> ions in the mass spectra of vapors over individual CeO<sub>2</sub> and the BaO–CeO<sub>2</sub> system has been discussed in detail elsewhere [9, 24].

The CeO<sub>2</sub><sup>+</sup> ion has a molecular origin and is formed by direct ionization of CeO<sub>2</sub> molecules, whereas CeO<sup>+</sup> has a dual origin: it is formed both by direct ionization of CeO molecules and by dissociative ionization of

CeO<sub>2</sub> molecules. Similarly, TiO<sub>2</sub><sup>+</sup> is a molecular ion, while TiO<sup>+</sup> is formed by both direct ionization of TiO molecules and dissociative ionization of TiO<sub>2</sub> molecules. Under isothermal conditions, the CeO<sup>+</sup>/CeO<sub>2</sub><sup>+</sup>

and TiO<sup>+</sup>/TiO<sub>2</sub><sup>+</sup> ion current ratios exhibited an increase, which is attributed to the partial thermal reduction of cerium and titanium in the condensed phase. Notably, the rate of increase of these ratios for the CeO<sub>2</sub>–TiO<sub>2</sub> system samples was lower than that observed for pure CeO<sub>2</sub> or TiO<sub>2</sub>. At high CeO<sub>2</sub> concentrations, oxygen released through reaction (3) stabilizes Ti(IV). Conversely, at high TiO<sub>2</sub> concentrations, Ce(IV) is stabilized. The stabilization of these oxidation states is attributed not only to oxygen release but also to the stabilization of the crystal lattice, which makes the transition to lower oxidation states less favorable. Due to the thermal instability of TiO<sub>2</sub>(s) at the experimental temperatures, pure TiO<sub>2</sub> cannot be used for activity determination. Upon heating, the partial pressure of TiO<sub>2</sub>(g) above TiO<sub>2</sub>(s) decreases rapidly, whereas the partial pressure of TiO(g) increases due to the reduction of Ti(IV) to Ti(III). Under these conditions, the application of equation (6) to determine TiO<sub>2</sub> activity would lead to unacceptably large uncertainties. Consequently, Ti<sub>3</sub>O<sub>5</sub> was chosen as the reference compound, as it does not change its phase composition upon heating and evaporates

congruently [25], making it suitable for determining the activity of titanium dioxide in the condensed phase. The applicability of this reference compound was previously validated in experiments determining TiO<sub>2</sub> activity in Ti<sub>3</sub>O<sub>5</sub> using TiO<sub>2</sub> as the standard state [26].

The activities of cerium dioxide in the concentration range of 10–90 mol % CeO<sub>2</sub> were determined by differential mass spectrometry using equation (5) with individual CeO<sub>2</sub> as the reference. Since individual TiO<sub>2</sub> exhibits significantly lower vapor pressure than CeO<sub>2</sub> at the experimental temperatures [18], experimental determination of TiO<sub>2</sub> activities at 2150 K using Eq. (6) was possible only for samples no. 1 and no. 2. In the homogeneous melt region at 2150 K, activities of TiO<sub>2</sub> for samples no. 1–7 were determined using the Gibbs–Duhem Eq. (8):

$$\ln \gamma(\text{TiO}_2) = - \int_{\ln \gamma_0(\text{CeO}_2)}^{\ln \gamma(\text{CeO}_2)} \frac{x(\text{CeO}_2)}{x(\text{TiO}_2)} d \ln \gamma(\text{CeO}_2), \quad (8)$$

where  $\gamma$  is the activity coefficient and  $x$  is the molar fraction of the component.

$$\gamma_i = \frac{a_i}{x_i}, \quad (9)$$

where  $a_i$  is the activity,  $\gamma_i$  is the activity coefficient, and  $x_i$  is the molar fraction of component  $i$ .

Integration was performed graphically with extrapolation to the infinite dilution [27].

Based on the obtained activity values, Gibbs energies and excess Gibbs energies over the entire investigated concentration range were calculated using Eqs. (10)–(13):

$$\Delta \mu_i = RT \ln a_i; \quad (10)$$

$$\Delta \mu_i^E = RT \ln \gamma_i; \quad (11)$$

$$\Delta G = \sum x_i \Delta \mu_i; \quad (12)$$

$$\Delta G^E = \sum x_i \Delta \mu_i^E. \quad (13)$$

**Table 3.** Activities, activity coefficients, Gibbs energies, and excess Gibbs energies in the CeO<sub>2</sub>–TiO<sub>2</sub> system at 2150 K

$x(\text{CeO}_2)$	$x(\text{TiO}_2)$	$a(\text{CeO}_2)$	$a(\text{TiO}_2)$	$\gamma(\text{CeO}_2)$	$\gamma(\text{TiO}_2)$	$-\Delta G^m$ , kJ/mol	$-\Delta G^E$ , kJ/mol
0.0	1.0	0	1	0	1	0	0
0.1	0.9	$0.006 \pm 0.005$	$0.81 \pm 0.07$	$0.062 \pm 0.05$	$0.90 \pm 0.08$	$12.4 \pm 2.0$	$6.6 \pm 2.0$
0.2	0.8	$0.033 \pm 0.007$	$0.61 \pm 0.03$	$0.163 \pm 0.035$	$0.76 \pm 0.04$	$19.4 \pm 1.1$	$10.5 \pm 1.1$
0.3	0.7	$0.083 \pm 0.007$	$0.44 \pm 0.16$	$0.278 \pm 0.023$	$0.63 \pm 0.022$	$23.5 \pm 0.6$	$12.6 \pm 0.6$
0.4	0.6	$0.159 \pm 0.011$	$0.312 \pm 0.014$	$0.397 \pm 0.028$	$0.52 \pm 0.024$	$25.7 \pm 0.7$	$13.6 \pm 0.7$
0.5	0.5	$0.257 \pm 0.025$	$0.209 \pm 0.020$	$0.51 \pm 0.05$	$0.42 \pm 0.04$	$26.1 \pm 1.2$	$13.7 \pm 1.2$
0.6	0.4	$0.38 \pm 0.04$	$0.131 \pm 0.021$	$0.63 \pm 0.07$	$0.33 \pm 0.05$	$25.0 \pm 1.6$	$13.0 \pm 1.6$
0.7	0.3	$0.515 \pm 0.027$	$0.072 \pm 0.009$	$0.74 \pm 0.04$	$0.24 \pm 0.03$	$22.4 \pm 0.9$	$11.5 \pm 0.9$
0.8	0.2	1.00	–	1.00	–	–	–
0.9	0.1	1.00	–	1.00	–	–	–
1.0	0.0	1	0	1	0	0	0

The results are summarized in the Table 3 and illustrated in Figs. 1 and 2.

The temperature dependence of cerium dioxide activity was examined in the range of 2100–2200 K within the homogeneous melt region. For all investigated samples,  $a(\text{CeO}_2)$  values were found to be temperature-independent within experimental uncertainty. For samples №8 and №9 with the highest CeO<sub>2</sub> content, the activity equals unity, indicating the presence of individual CeO<sub>2</sub> phase at 2150 K.

For sample No. 2, the activity of titanium dioxide was additionally determined directly using Eq. (6). Determining these values experimentally for the remaining samples was impossible, as the partial pressure of TiO<sub>2</sub> over these samples within the studied temperature range fell below the instrument's detection limit. The close agreement between the values obtained by the two independent methods serves as a key criterion for the reliability of the results.

The obtained data indicate that the CeO<sub>2</sub>–TiO<sub>2</sub> system at 2150 K exhibits a negative deviation from

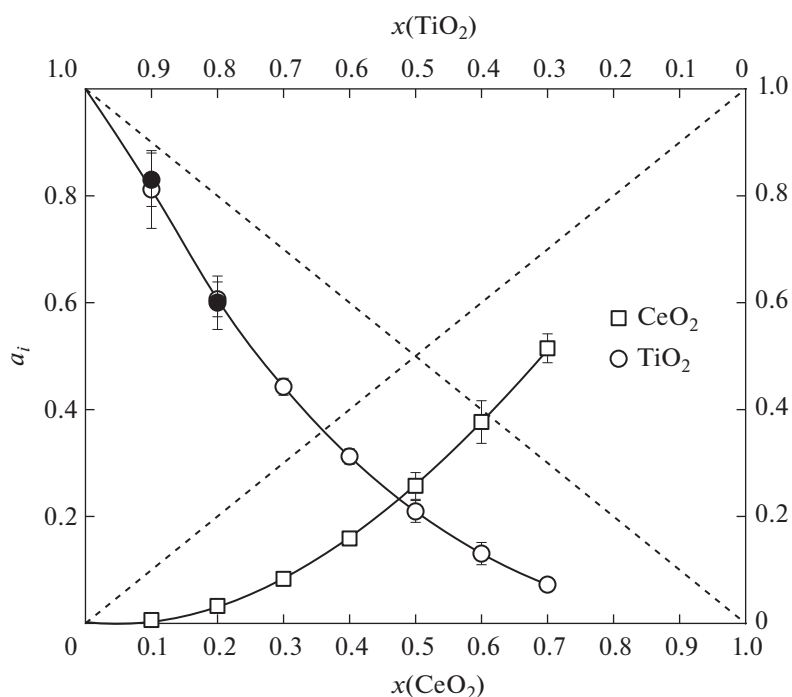


**Fig. 1.** Dependence of CeO<sub>2</sub> and TiO<sub>2</sub> activities on composition in the CeO<sub>2</sub>–TiO<sub>2</sub> system at 2150 K. The TiO<sub>2</sub> activity values obtained directly by the differential method are marked with black circles.

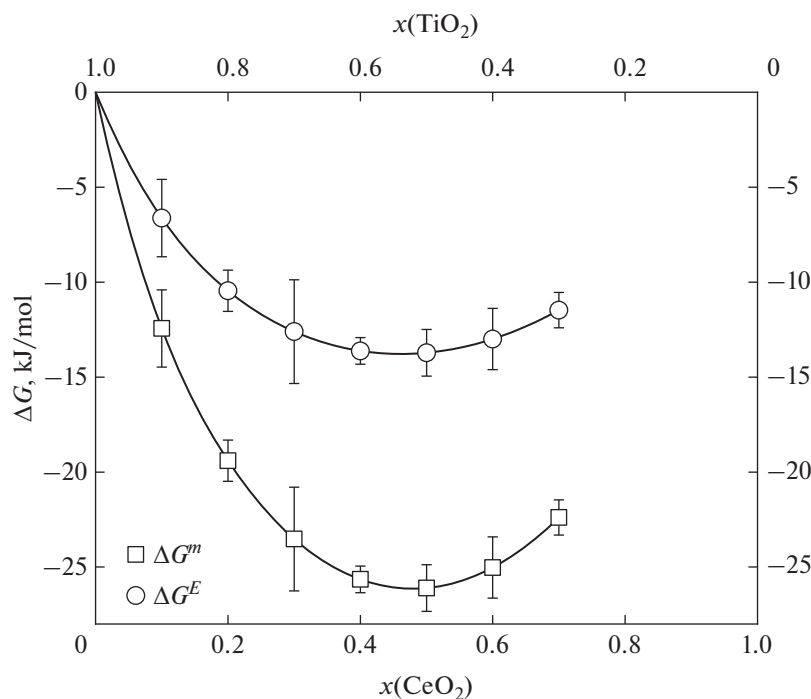


**Fig. 2.** Dependence of the molar Gibbs energy of mixing ( $\Delta G^m$ ) and the excess Gibbs energy ( $\Delta G^E$ ) on composition for the  $\text{CeO}_2$ – $\text{TiO}_2$  system at 2150 K.

Raoult's law for both components, indicating significant interactions in the melt.

### CONCLUSIONS

Samples of the  $\text{CeO}_2$ – $\text{TiO}_2$  system with  $\text{CeO}_2$  contents ranging from 10 to 90 mol % were synthesized by the ceramic method. After annealing at 1400°C for 22.5 h, all samples were found to contain a stable  $\text{CeTi}_2\text{O}_6$  phase, with its fraction varying from 9 to 78% depending on initial composition.

At 2150 K, most of the samples fall within the homogeneous melt region, which made it possible to determine the thermodynamic properties of the system over a wide range of melt compositions.

It was established that  $\text{CeO}_2$  stabilizes  $\text{TiO}_2$  at high temperatures, reducing the rate of thermal reduction. The excess Gibbs energies of mixing reach  $-13.7$  kJ/mol, confirming the thermodynamic stability of the system.

The melting temperatures of the samples range from 1723 to 2493°C and show a clear dependence on composition. The composition dependence of component activities confirms homogeneous melting. Samples with high  $\text{CeO}_2$  contents (80–90 mol %) exhibit cerium dioxide activities close to unity, which indicates the presence of an individual  $\text{CeO}_2$  phase at 2150 K.

The investigation of the thermodynamic properties of the  $\text{CeO}_2$ – $\text{TiO}_2$  system has revealed key patterns of

its high-temperature behavior. The formation of the stable  $\text{CeTi}_2\text{O}_6$  phase and the negative deviations from ideality in the melt indicate a significant interaction between the components of the system, which is crucial for the development of ceramic materials with enhanced performance characteristics. The obtained data on activities, Gibbs energies, and melting temperatures provide a foundation for modeling the synthesis and degradation processes of  $\text{CeO}_2$ – $\text{TiO}_2$ -based materials under high-temperature conditions. These results advance the understanding of the high-temperature behavior of complex oxide systems and can be utilized for the design of materials with controlled properties.

### ACKNOWLEDGMENTS

The authors are grateful to the Cryogenic department of the Science Park of St. Petersburg State University for the uninterrupted supply of liquid nitrogen. The XRD and XRF data were obtained at the Research Centers for X-Ray Diffraction Studies, chemical analysis, and materials and physical methods of surface investigation, respectively. All the research centers used are departments of the Science Park at St. Petersburg State University.

### FUNDING

The work was carried out within the framework of the Russian Science Foundation (Project no. 24-23-00047).

“High temperature thermodynamic study of ceramics system based on ceria.”

#### CONFLICT OF INTEREST

The authors of this work declare that they have no conflicts of interest.

#### REFERENCES

1. M. J. Muñoz-Batista, A. Kubacka, M. N. Gómez-Cerezo, et al., *Appl. Catal., B* **140–141**, 626 (2013). <https://doi.org/10.1016/j.apcatb.2013.04.071>
2. J. R. Sivalingam, F. K. Chong, and C. D. Wilfred, *Bull. Chem. React. Eng. Cat.* **13**, 170 (2018). <https://doi.org/10.9767/bcrec.13.1.1396.170-178>
3. Y. Zhu, G. Li, S. Zhang, et al., *Electrochim. Acta* **56**, 7550 (2011). <https://doi.org/10.1016/j.electacta.2011.06.091>
4. J. Wang, J. Sun, Q. Jing, et al., *J. Eur. Ceram. Soc.* **38**, 2841 (2018). <https://doi.org/10.1016/j.jeurceramsoc.2018.02.019>
5. W. O. Groves, M. Hoch, and H. L. Johnston, *J. Phys. Chem.* **59**, 127 (1955). <https://doi.org/10.1021/j150524a008>
6. J. Drowart, P. Coppens, and S. Smoes, *J. Chem. Phys.* **50**, 1046 (1969). <https://doi.org/10.1063/1.1671099>
7. D. L. Hildebrand, *Chem. Phys. Lett.* **44**, 281 (1976). [https://doi.org/10.1016/0009-2614\(76\)80510-6](https://doi.org/10.1016/0009-2614(76)80510-6)
8. H. Y. Wu and P. G. Wahlbeck, *J. Chem. Phys.* **56**, 4534 (1972). <https://doi.org/10.1063/1.1677900>
9. S. I. Lopatin, S. M. Shugurov, and A. I. Panin, *Rapid Commun. Mass Spectrom.* **30**, 2027 (2016). <https://doi.org/10.1002/rcm.7677>
10. V. Piacente, G. Bardi, L. Malaspina, et al., *J. Chem. Phys.* **59**, 31 (1973). <https://doi.org/10.1063/1.1679807>
11. H. G. Staley and J. H. Norman, *Int. J. Mass Spectrom. Ion Phys.* **2**, 35 (1969). [https://doi.org/10.1016/0020-7381\(69\)80004-5](https://doi.org/10.1016/0020-7381(69)80004-5)
12. P. W. Gilles, K. D. Carlson, H. F. Franzen, et al., *J. Chem. Phys.* **46**, 2461 (1967). <https://doi.org/10.1063/1.1841070>
13. O. Y. Kurapova, S. M. Shugurov, E. A. Vasil'eva, et al., *J. Alloys Compd.* **776**, 194 (2019). <https://doi.org/10.1016/j.jallcom.2018.10.265>
14. S. M. Shugurov, O. A. Zhinkina, E. A. Balabanova, et al., *Ceram. Int.* **51**, 7202 (2025). <https://doi.org/10.1016/j.ceramint.2024.12.154>
15. O. Y. Kurapova, S. M. Shugurov, E. A. Vasil'eva, et al., *Ceram. Int.* **47**, 11072 (2021). <https://doi.org/10.1016/j.ceramint.2020.12.230>
16. S. I. Lopatin, S. M. Shugurov, and O. Y. Kurapova, *Russ. J. Gen. Chem.* **91**, 2008 (2021). <https://doi.org/10.1134/S1070363221100121>
17. N. A. Toropov, E. K. Keler, A. I. Leonov, et al., *Bull. Acad. Sci. USSR* **32**, 46 (1962).
18. L. V. Gurvich, I. V. Veits, V. A. Medvedev, et al., *Thermodynamic Properties of Individual Substances: Handbook*, vol. 3, book 2, Ed. by V. P. Glushko (Nauka, Moscow, 1981) [in Russian].
19. E. K. Kazenas and Yu. V. Tsvetkov, *Evaporation of Oxides* (Nauka, Moscow, 1997) [in Russian].
20. A. Galtayries, R. Sporken, J. Riga, et al., *J. Electron. Spectrosc. Relat. Phenom.* **88–91**, 951 (1998). [https://doi.org/10.1016/S0368-2048\(97\)00134-5](https://doi.org/10.1016/S0368-2048(97)00134-5)
21. M. Daturi, C. Binet, J. C. Lavalley, et al., *Phys. Chem. Chem. Phys.* **1**, 5717 (1999). <https://doi.org/10.1039/A905758G>
22. M. S. P. Francisco, V. R. Mastelaro, P. A. P. Nascente, et al., *J. Phys. Chem. B* **105**, 10515 (2001). <https://doi.org/10.1021/jp0109675>
23. S. G. Lias, J. E. Bartmess, J. F. Liebman, et al., *J. Phys. Chem. Ref. Data* **17**, Suppl. 1 (1988).
24. S. I. Lopatin, S. M. Shugurov, A. I. Panin, et al., *Rapid Commun. Mass Spectrom.* **31**, 1559 (2017). <https://doi.org/10.1002/rcm.7931>
25. P. G. Wahlbeck and P. W. Gilles, *J. Chem. Phys.* **46**, 2465 (1967). <https://doi.org/10.1063/1.1841071>
26. S. I. Lopatin, S. M. Shugurov, Z. G. Tyurnina, et al., *Glass Phys. Chem.* **47**, 38 (2021). <https://doi.org/10.1134/S1087659621010077>
27. L. N. Sidorov, M. V. Korobov, and L. V. Zhuravleva, *Mass-Spectrometric Thermodynamic Studies* (Moscow University Press, Moscow, 1985) [in Russian].

**Publisher's Note.** Pleiades Publishing remains neutral with regard to jurisdictional claims in published maps and institutional affiliations. AI tools may have been used in the translation or editing of this article.